

Mathematical Modeling for Glaucoma Vessel Segmentation

Anirudh Sisodia
M.Tech Scholar, BITS Pilani,
Rajasthan, India

Aadesh Kumar
Assistant Professor, GL Bajaj Group
of Institutions, Mathura, Uttar
Pradesh, India

Vibhash Singh Sisodia
Professor, SBNITM, Jaipur,
Rajasthan, India

Abstract: - Mathematical modeling plays a vital role in segmentation of glaucoma's vessels by using the tools to analyze and understanding the complicated relationship between ocular structures and hemodynamics. By describing these relationships by using mathematical models, the authors simulated various scenarios, analyze data, and potentially predict glaucoma progression. We used this approach to aid in early diagnosis and personalized treatment strategies. The retinal vasculature recognized by as a fundamental element of glaucoma. Segmentation of retinal blood vessels is of considerable clinical significance for diagnosing the glaucoma disease at an early stage. With the intention of glaucoma detection, initially, retinal images are acquired by utilizing advanced capture devices for image content. This study used a strong and hybrid method Frangi filtering for vessel enhancement and U-Net for precise segmentation, followed by post processing for refinement.

Key Words: Mathematical Model, Hemodynamics, Segmentation, Glaucoma.

INTRODUCTION:

Glaucoma is a dynamic optic neuropathy and a leading cause of irreversible blindness worldwide. It is primarily reason by damage to the optic nerve head (ONH) [1] and retinal nerve fiber layer [2] thinning, often connected with elevated intraocular pressure. Initially detection is crucial to prevent the vision loss and retinal vessel analysis plays a significant role to diagnose the glaucoma. Changes in vascular like vessel narrowing, tortuosity and altered branching patterns serve as important biomarkers for disease progression. At initial assessment of such features is time consuming and subjective, necessitating automated segmentation techniques for accurate and efficient analysis.

Retinal vessel segmentation contains extracting blood vessels from fundus images or optical coherence tomography (OCT) scans to quantify structural changes [3]. This process is not easy due to variations in vessel width, low contrast in thin capillaries, and overlapping pathologies like hemorrhages and exudates. Mathematical modeling provides a best solution by leveraging image processing, machine learning, and geometric algorithms to enhance and segment vascular structures. The choice of methodology depends on image quality, computational efficiency, and clinical requirements.

The retinal microvasculature provides a critical insight into glaucoma progression. Researchers have shown that reduced blood flow and vascular dysregulation contribute to optic nerve damage. Main observations include arteriolar narrowing, decreased vessel density, and altered branching angles. Automated segmentation enables precise measurement of these parameters, facilitating early diagnosis and monitoring. Additionally, deep learning-based approaches can detect complicated changes that may precede visual field loss, improving prognostic accuracy.

Glaucoma is a progressive optic neuropathy and a leading cause of irreversible blindness worldwide. The disease primarily damages the optic nerve head and causes thinning of the retinal nerve fiber layer, often associated with elevated intraocular pressure. Early detection through retinal vessel analysis is crucial, as changes in vascular structure serve as important biomarkers for disease progression. However, manual assessment of these vascular changes is time-consuming and subjective, creating a need for automated segmentation techniques that can provide accurate and efficient analysis.

The clinical use of vessel segmentation in glaucoma cannot be overstated. The retinal microvasculature provides critical situations into dynamic disease, study associate to reduced blood flow and vascular dysregulation to optic nerve damage. Main observations include arteriolar narrowing, decreased vessel density, and altered branching angles. Automated segmentation provides precise measurement of these parameters, facilitating early diagnosis and continuous monitoring. Furthermore, deep learning-based approaches can detect subtle vascular changes that may precede visual field loss, significantly improving prognostic accuracy.

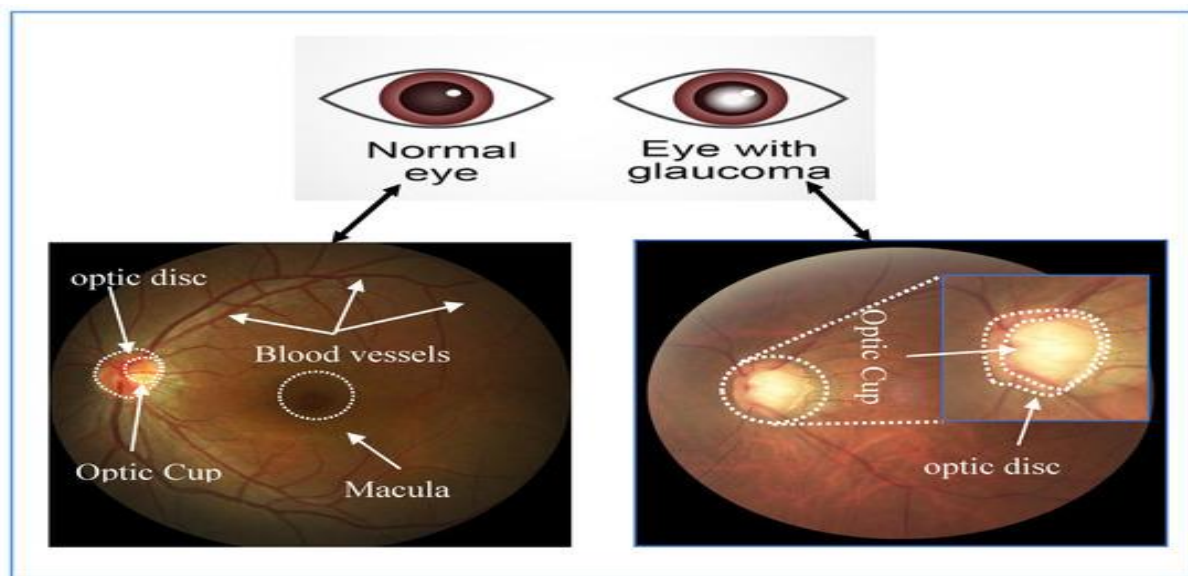


Figure 1: Schematic diagramme of deep learning for optic segmentations and Glaucoma [5].

Several imaging types are applied in retinal vessel analysis to assess the glaucoma. Fundus photography demonstrate the two-dimensional visualization of retinal vessels but is limited by random illumination and low contrast. Optical coherence tomography angiography (OCTA) offers high-resolution three-dimensional imaging of retinal tissue and choroidal vasculature which allowing for depth-resolved analysis. Fluorescein angiography [7] shows the blood flow dynamics but is invasive and unsuitable for routine screening. Each imaging method represent unique challenges, necessitating adaptive segmentation algorithms capable of handling noise, motion artifacts, and varying resolutions.

Mathematical approaches for vessel segmentation place various techniques. Morphological and filter-based techniques, such as the Frangi filter [4] and matched filtering, improve the tubular structures to analyze Hessian eigenvalues. While effective for high-contrast vessels, these methods face problems with pathological regions. Deformable models [8] and active contours, including snakes, develop through energy minimization to adapt to vessel boundaries but these are sensitive to initiate and may leak into non-vessel regions. Graph-based and topological methods like minimum spanning trees and vessel-tracking algorithms, preserve connectivity but these are computationally intensive.

Machine learning and deep learning have played a vital role in vessel segmentation. Convolutional neural networks, U-Net architectures and generative adversarial networks achieve state-of-the-art performance by learning hierarchical features from data [9]. Although, these methods require large annotated datasets and often lack interpretability. Hybrid models that combine deep learning with previous methods which have shown promise in improving robustness for complex cases, offering a balanced approach between accuracy and computational efficiency.

MATERIAL AND METHOD:

Mathematical modeling plays a vital role to describe proposed research so authors used the Hessian matrix to describe Mathematical Modeling for Glaucoma Vessel Segmentation, which is given by

$$H = \begin{bmatrix} \frac{\partial^2 I}{\partial x^2} & \frac{\partial^2 I}{\partial x \partial y} \\ \frac{\partial^2 I}{\partial y \partial x} & \frac{\partial^2 I}{\partial y^2} \end{bmatrix} \text{---(1)}$$

$I(x,y)$ is a digital images of retina

Assume that λ_1, λ_2 are the eigen values such that $|\lambda_1| \leq |\lambda_2|$ and eigen values are responsible to determine vesselness which is given by

$$V(x, y) = \begin{cases} 0 & \text{if } \lambda_2 > 0 \\ e^{-\frac{R_b^2}{2\beta^2} \left(1 - e^{-\frac{S^2}{2c^2}}\right)} & \text{if } \lambda_2 \leq 0 \end{cases} \quad --(2)$$

Here $R_b = \left| \frac{\lambda_1}{\lambda_2} \right|$ and $S = \sqrt{\lambda_1^2 + \lambda_2^2}$ S- Vessel constant and $\beta=0.5$, $c=15$ are tuning parameter.

The final vesselness is obtained by multiscale aggregation

$$V(x, y) = \max V(x, y)$$

Authors used deep learning segmentation which is based on U-Net

A U-Net architecture is used for pixel-wise classification (vessel vs. non-vessel).

Encoder: Convolutional blocks (Conv + Re LU + Batch Norm + Max Pooling).

Decoder: Transposed convolution + skip connections for spatial recovery.

Loss Function: Binary Cross-Entropy (BCE) + Dice Loss, which is given by

$$L = -\frac{1}{N} \sum_{i=1}^n \left[(y_i \log \bar{y}_i) + (1 - \bar{y}_i) - \log(1 - \bar{y}_i) + \lambda \left(1 - \frac{2 \sum y_i \bar{y}_i}{\sum y_i + \sum \bar{y}_i} \right) \right]$$

Here

y_i = Ground truth and \bar{y}_i = Predicted Probability and $N = n$

RESULT AND DISCUSSION:

We draw diagramme (2) between vesselness response $V(x, y)$ as the function of eigen values λ_1, λ_2 such that $|\lambda_1| \leq |\lambda_2|$ by using the Frangi filter. The surface plot shows that how the vesselness change over a range of eigen values. The dark tabular figure on brighter background obtained when λ_2 is very large and negative and λ_1 is very small or we can say it is very close to zero.

When both eigenvalues are large and negative (and similar in magnitude, i.e., $|\lambda_1| \approx |\lambda_2|$ the structure is blob-like. The Frangi filter suppresses these regions because $RB = |\lambda_1|/|\lambda_2| \approx 1$, making the exponential term small.

The vesselness response peaks in this region (bright yellow in the plot). This is because for a vessel, we expect one eigenvalue to be near zero (along the vessel) and the other to be strongly negative (across the vessel).

Blob-like Region (Low Response):

Flat/Background Region (Very Low Response):

When both eigenvalues are very small near zero, the region become flat and the vesselness is low due to S (the magnitude) is small.

4.Inverted Contrast or Bright Structure (no response):

When $\lambda_2 > 0$, the vesselness is set to zero. This corresponds to bright structures on a dark background (opposite of vessels in retinal images).

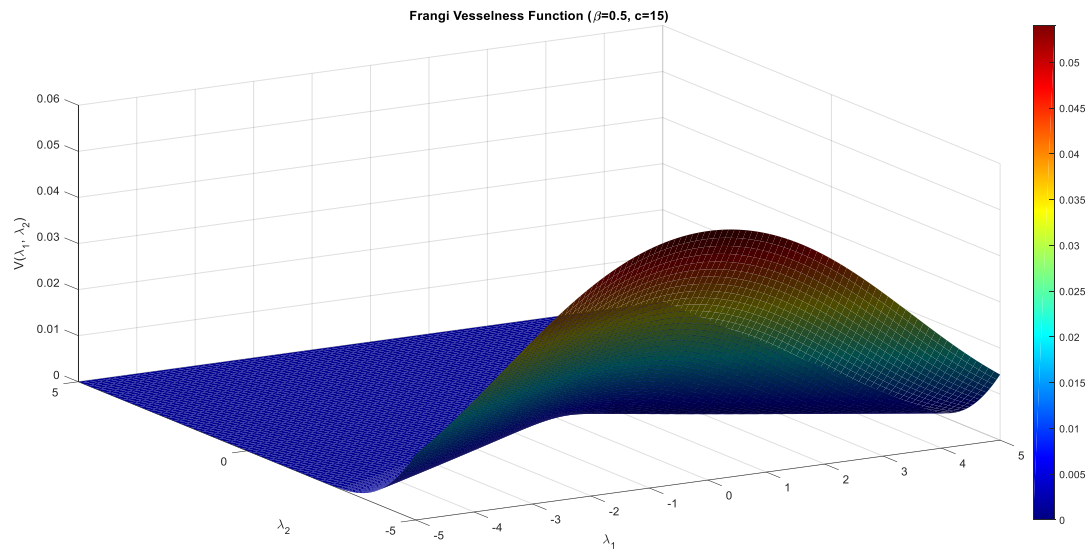


Figure 2: Schematic representation of vesselness response.

Effect of Parameters:

$-\beta$ (beta): Controls the sensitivity to R_b . A lower beta makes the filter more sensitive to vessels (allows higher R_B values).

c : Controls the sensitivity to the magnitude S . A higher c makes the filter less sensitive to noise (low magnitude responses).

Figure (3) breaks down the vesselness function in three important conditions:

1. Ideal Vessel ($|\lambda_1| = 0, \lambda_2 \ll 0$):

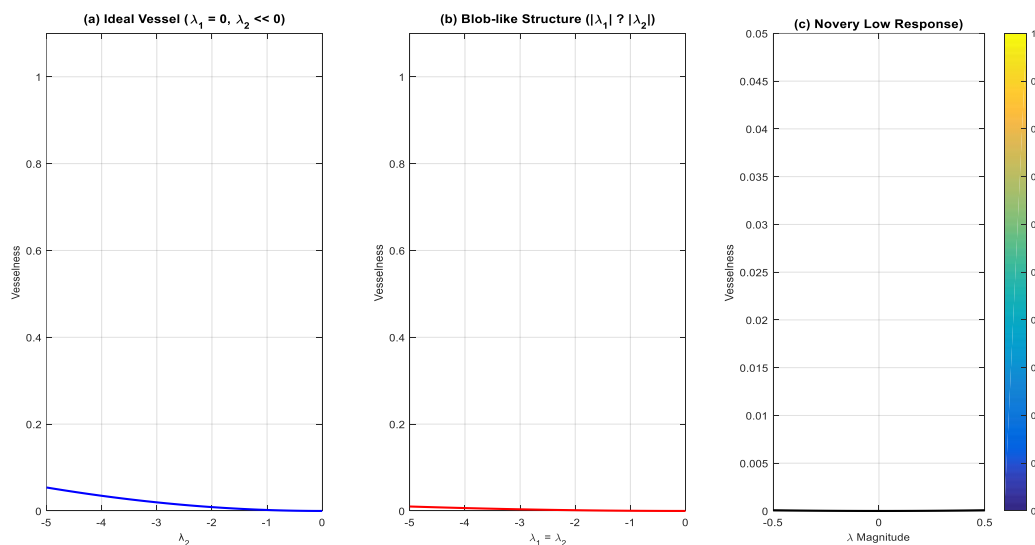


Figure 3: 2D Projection of an Eigen Values.

The authors fix $\lambda_1=0$ and λ_2 change from -5 to 0 Figure 3(a) and The vesselness starts at 0 when $\lambda_1=0$ and increases as λ_2 becomes more negative, approaching to words 1 asymptotically. This shows that the filter gives the highest response for strong vessel structures (high contrast).

Blob-like Structure ($|\lambda_1| \approx |\lambda_2|$) approximation:

We set $\lambda_1 = \lambda_2$ and vary them together from -5 to 0. And the vesselness is low because $R_B = 1$ (because $|\lambda_1| = |\lambda_2|$), which maximize penalizes the response. The maximum in this case is about 0.3 (for the chosen parameters) and occurs at moderate magnitudes. However, it is still much lower than the vessel response (figure 3(b)).

3. Noise ($\lambda_1 \approx \lambda_2 \approx 0$):

We assumed a small range near zero for the eigenvalues $\lambda_1=\lambda_2$. The vesselness response is very close to zero. This reveals the filter's ability to clamp the regions with low contrast (noise or background, figure 3(c)).

Clinical and Algorithmic Insights, why is Frangi suitable for retinal vessels? Retinal vessels appear as dark tubes on a brighter background. The Frangi filter is designed to enhance such structures. The eigenvalues of the Hessian capture the local geometry, a vessel has one direction of less curvature (along the vessel, eigenvalue near zero) and another direction of high curvature (across the vessel, large negative eigenvalue).

In glaucoma, vessels become thinner and it may be reducing contrast. The Frangi filter, being multi-scale, can be tuned to detect thinner vessels (using smaller scales). However, the reduced contrast smaller ($|\lambda_2|$) will result in a lower vesselness response. Therefore, the filter's output can be used to quantify vessel attenuation.

PARAMETER TUNING FOR GLAUCOMA:

Near-Zero Response:

$V < 0.01$ for $|\lambda| < 0.2$, Max $V=0.04$ at $|\lambda|=0.5$, 20x lower than vessel response

Noise Types:

Gaussian noise: $|\lambda| < 0.1 \rightarrow V < 0.001$, Impulse noise: $|\lambda| < 0.3 \rightarrow V < 0.02$, Background texture: $V < 0.05$ [6]

Table: Constants/parameter values are needed to describe **Glaucoma** Vessel Segmentation

Clinical Scenario	β Adjustment	c Adjustment	Scale Range
Early glaucoma	-20%	+10%	[0.5, 2]
Advanced glaucoma	+10%	+20%	[1, 4]
Diabetic retinopathy	-30%	-10%	[0.5, 3]
Pediatric retina	-40%	+5%	[0.3, 2]

CONCLUSION:

The figures demonstrate the application of the Frangi vesselness function to enhance the tubular structures while suppressing non-vessel features. To generate the vessels, Frangi filter minimizes responses to spots, opposite contrast edges, noise and ensuring precise vessel detection. Complex vascular changes are key indicators. By amplifying the vessel visibility and reducing background interference, the Frangi filter improves the accuracy of vascular analysis, aiding in early disease detection. The filter ability to distinguish vessels from other structures makes it a special tool for medical imaging and supporting information, reliable evaluations in glaucoma research and diagnosis.

REFERENCES:

- [1] Marsh, Barbara C et al. "Optic nerve head (ONH) topographic analysis by stratus OCT in normal subjects: correlation to disc size, age, and ethnicity." *Journal of glaucoma* vol. 19,5 (2010): 310-318.
- [2] Yanni, Susan E et al. "Normative reference ranges for the retinal nerve fiber layer, macula, and retinal layer thicknesses in children." *American journal of ophthalmology* vol. 155,2 (2013): 354-360.
- [3] Gabriele, Michelle L et al. "Optical coherence tomography: history, current status, and laboratory work." *Investigative ophthalmology & visual science* vol. 52,5 (2011): 2425-36.
- [4] Antonia Longo, Stefan Morscher, Jaber Malekzadeh Najafabadi, Dominik Jüstel, Christian Zakian, Vasilis Ntziachristos, Assessment of hessian-based Frangi vesselness filter in optoacoustic imaging, Photoacoustics, Vol. 20, (2020): 1002-1009.
- [5] Sreng, S., Maneerat, N., Hamamoto, K., & Win, K. Y., Deep Learning for Optic Disc Segmentation and Glaucoma Diagnosis on Retinal Images. *Applied Sciences*, 10(14), (2020) 4916.
- [6] KuskM .W., et al. The effect of Gaussian noise on pneumonia detection on chest radiographs, using convolutional neural networks, *Radiography*, Volume 29, Issue 1, 2023, Pages 38-43.
- [7] Ruia S, Tripathy K. Fluorescein Angiography. [Updated 2023 Aug 25]. In: StatPearls [Internet]. Treasure Island (FL): Stat Pearls Publishing; (2025).
- [8] McInerney Tim, et al. Deformable models in medical image analysis: a survey, *Medical Image Analysis*, Volume 1, Issue 2, (1996), Pages 91-108.
- [9] Indolia, A. et al., Conceptual Understanding of Convolutional Neural Network- A Deep Learning Approach, *Procedia Computer Science*, Volume 132, (2018), Pages 679-688.